

Thermal Response of the Multiplier of an Accelerator Driven System to Beam Interruptions

Floyd E. Dunn
Argonne National Laboratory
9700 S. Cass Avenue
Argonne, IL 60439
Phone: (630) 252-4692
Fax: (630) 252-4500
E-mail: fedunn@anl.gov

Abstract: Thermal response of the multiplier of an accelerator driven system to beam trips has been calculated for sodium cooled and lead-bismuth cooled multipliers. The temperature transients caused by a beam trip lead to thermal fatigue in structural components, and restoring the beam causes an additional temperature transient that adds to thermal fatigue. Design lifetimes for various multiplier components are calculated, based on the frequency of beam interruptions and on the thermal fatigue per interruption. Mitigation strategies to increase design lifetimes are discussed.

I. INTRODUCTION

A beam trip in an accelerator driven system leads to rapid temperature transients in the various parts of the multiplier. These temperature transients lead to thermal fatigue which limits the lifetimes of structural components. This paper discusses temperature transients in the multiplier, thermal fatigue and resulting limits on component lifetimes, and mitigation measures to improve component lifetimes.

II. DESCRIPTION OF MULTIPLIER CONCEPTS

Three multiplier concepts are used in this paper. The first multiplier is based on the Advanced Liquid Metal Reactor (ALMR) concept¹. This concept was used in the Accelerator Transmutation of Waste (ATW) report to Congress². This concept uses metal fuel and sodium coolant, and it has a nominal power level of 840 MWt. This concept is shown in Figure 1. The accelerator beam strikes a target in the middle of the multiplier core. The multiplier power is produced in the target and the core.

Coolant flows upward through the core into the outlet plenum. From there the coolant goes to the shell side of a shell-and-tube intermediate heat exchanger (IHX) where it transfers its heat to the intermediate coolant loop. The primary coolant then goes to the cold pool. Coolant from the cold pool is sucked by the pump and pumped into the inlet plenum, from which it goes through the core. The intermediate coolant loop carries the heat to the steam generator.

The second multiplier concept is similar to the first, but lead-bismuth is used for the coolant instead of sodium. There is no intermediate loop in this concept. Instead, the steam generator is placed where the intermediate heat exchanger would be. In order to avoid excessive coolant pressure drop through the core, and to avoid corrosion of the steel by lead-bismuth, the coolant flow velocity through the core is limited by providing a larger flow area per pin in the core subassemblies. With lead-bismuth coolant one row of pins is removed from the subassembly, leaving 169 pins per subassembly instead of the 217 pins used with sodium. For both of the first two concepts the coolant temperature rise in the hottest core

channel is 164 K, and the average coolant temperature rise is 139 K.

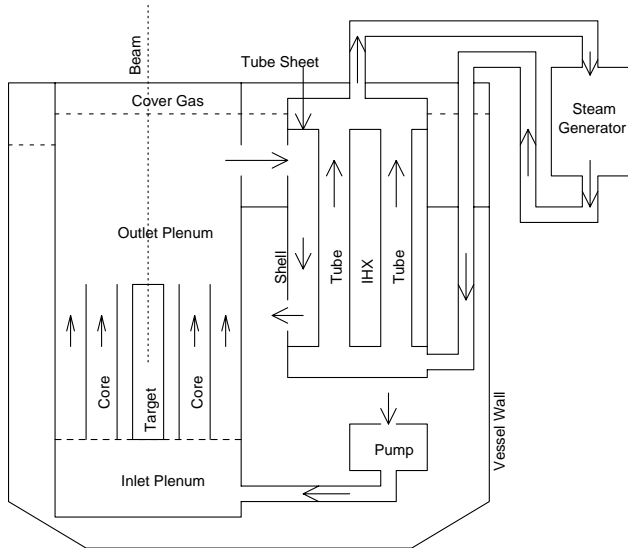


Fig. 1, Schematic of Multiplier Coolant Flow

The third multiplier concept is the Subcritical Multiplier (SCM-100) used with the Accelerator Driven Test Facility (ADTF). This concept is based on the EBR-II reactor, scaled up to 100 MWt from 62.5 MWt. Thus, this concept is significantly smaller than the first two. The third multiplier concept also uses metal fuel and sodium coolant. In addition, in the third concept there is a cover on the outlet plenum and a pipe from the outlet plenum to the IHX. In this concept the average coolant temperature rise across the core is 100 K.

III. ANALYSIS METHODS

In order to analyze the consequences of a beam loss and return to power transient, the SASSYS-1 LMR systems analysis code³ was used to obtain the time dependent temperatures of the coolant in contact with various structural components. Multi-node structural temperature calculations were then used to obtain minimum, maximum and average structure temperatures. The difference between the minimum or maximum temperature and the average structure temperature was multiplied by the thermal expansion coefficient to obtain the strain

magnitude. The peak strain magnitude was used with the American Society of Engineers (ASME) Boiler and Pressure Vessel Code⁴ to determine the allowable number of cycles the structural component can be subjected to. Beam reliability data⁵ for the LANSCE accelerator were used to obtain the number of beam interruptions per year of a particular duration. The integral over interruption duration of the ratio of the interruptions per year for a particular interruption duration to the allowable number of cycles of that duration gave a damage function which determined the allowable lifetime for the structural component.

The SASSYS-1 LMR systems analysis code contains neutron kinetics coupled with a detailed thermal hydraulics treatment of the core, the primary and intermediate heat removal loops, and the steam generators. Both steady-state and transient calculations are done by the code. The neutron kinetics treatment contains point kinetics, with or without an external source. Also in the code is an optional 3-D time dependent neutron kinetics capability.

The method used for evaluation of low cycle fatigue at elevated temperatures is based on article T-1432 of Appendix T of Subsection NH of the ASME Boiler and Pressure Vessel Code. This type of analysis is required when the temperatures exceed 700 or 800 °F. The difference between the average structure temperature and the minimum or maximum temperature is multiplied by the thermal expansion coefficient to obtain the strain. The peak strain for a cycle is used to obtain the allowable number of cycles that the structure can be subjected to. Figure 2 shows results for 304 stainless steel. Note that an increase of only a few degrees in peak temperature difference can lead to a decrease of a factor of two in the allowable number of cycles.

Evaluation of low cycle fatigue in the HT-9 steel alloy used for cladding, subassembly duct walls, and shielding in the subassemblies is a special problem. Appendix T only includes data for four materials: 304 stainless steel, 316

stainless steel, Ni-Fe-Cr alloy 800H, and 2 ¼ Cr 1 Mo steel. Furthermore, there appears to be no low cycle fatigue failure data anywhere for HT-9. What is done in this work is to evaluate HT-9 as if it were 316 stainless steel and then divide the allowable number of cycles by an uncertainty factor. In order to estimate the uncertainty factor, the ASME low cycle fatigue treatment in Subsection NB of Section III is used. This treatment is limited to temperatures below 700 – 800 °F; but it is applicable to broad classes of steels, including one category for ferritic steels and another category for austenitic steels such as 316 stainless steel. Using this treatment the allowable number of cycles for the austenitic category tends to be about six times as great as the allowable number of cycles for the ferritic category with the same temperature difference. Therefore, a value of six is used for the uncertainty factor. Until fatigue data for HT-9 is available, there will be a significant uncertainty in the results for this material.

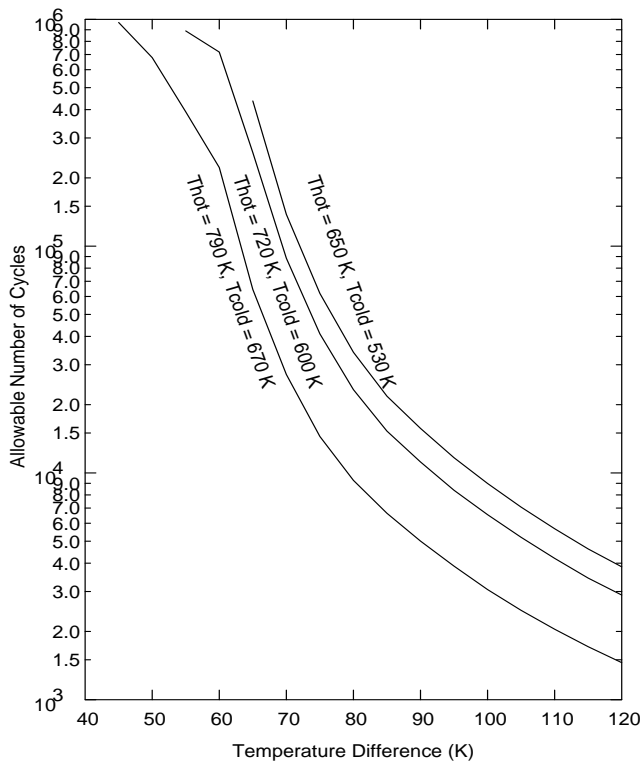


Fig. 2, ASME Thermal Fatigue Results

The data obtained by Eriksson for the frequency of beam interruptions of various durations in the LANSCE accelerator is shown in Table 1. This data is used as a reference point in calculating component lifetime. Compared to LANSCE, a new proton accelerator would probably be at least a factor of ten more reliable. One question to be addressed is whether a factor of ten improvement is sufficient.

Table 1, LANSCE Data for the Frequency of Beam Interruptions

Duration of interruption	Interruptions per day	Interruptions per year
10 seconds or more	39	14,200
1 minute or more	9.5	3482
2 minutes or more	5.5	2019
3 minutes or more	4.4	1597
4 minutes or more	4.0	1402
5 minutes or more	3.4	1237
15 minutes or more	1.7	617
1 hour or more	.6	214
5 hours or more	.09	34

In order to evaluate the allowable component lifetime, a damage rate, d , is used to give the damage per year. The allowable lifetime is $1/d$ years. To evaluate the damage rate for a wide range of interruption durations, the interruption durations are grouped into intervals. Interval i includes interruptions with down times from t_{di} to t_{di+1} . Then the damage rate is given by

$$d = \sum I_i/A_i$$

where

A_i = allowable number of cycles for interruptions in interval i , and

I_i = interruptions per year in interval i .

IV. TEMPERATURE TRANSIENTS

Analysis of the three multiplier concepts has shown where the critical structures are as far as thermal fatigue is concerned. For the sodium

cooled ATW, the critical areas are the above core load pads on the subassembly duct walls and the outer rim of the upper tube sheet in the intermediate heat exchanger. For the lead cooled ATW the critical area is the upper tube sheet of the steam generator. For the sodium cooled ADF the critical areas are the shielding inside the subassembly above the core and the outer rim of the upper tube sheet of the intermediate heat exchanger. Results for some of these critical areas are given in the sections below.

The normalized multiplier power after a beam trip is shown in Figure 3 for different values of the criticality, keff. The coolant pumps are assumed to continue operating after the beam trip, so the coolant flow continues at its initial value. The power drops almost instantaneously to 16% or 9%, depending on the criticality. Then the power drops gradually toward decay heat levels. Note that a lower criticality gives a more severe initial power transient. These results were calculated for the first multiplier concept, but similar results would be obtained for the other concepts.

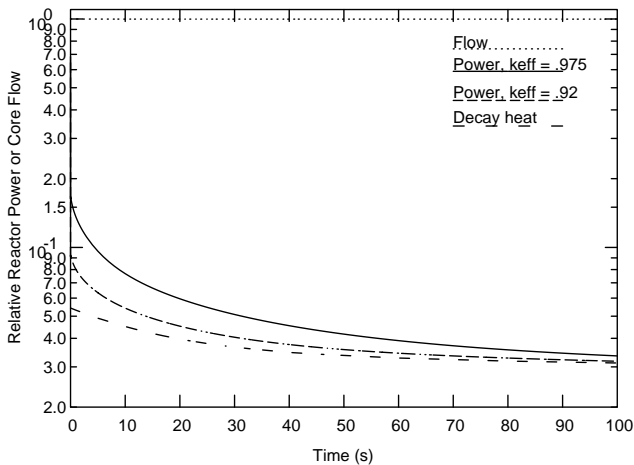


Fig. 3, Normalized Multiplier Power and Coolant Flow following a Beam Trip

Figure 4 shows the subassembly wall temperatures and coolant temperatures following a beam interruption for the sodium cooled ATW concept. These temperatures are at the location of the above-core load pads. At this location the subassembly duct wall is thickened to provide

spacing between subassemblies and to provide more strength at the point where the subassemblies are clamped together to limit lateral motion. In this case the wall surface temperature follows the coolant temperature closely, whereas the average wall temperature lags significantly. Figure 5 shows the difference between the average wall temperature and the wall surface temperature. This difference peaks at about 66 K two seconds after the beam interruption. Using the methods of the previous section, a 66 K temperature difference peak in HT-9 steel gives 7500 as the allowable number of cycles for this transient, without accounting for additional thermal fatigue due to the return to power. The LANSCE data would give a duct wall lifetime of about .53 years for this case. Since it is desirable to operate subassemblies for three or four years before they are replaced, this is not an acceptable lifetime.

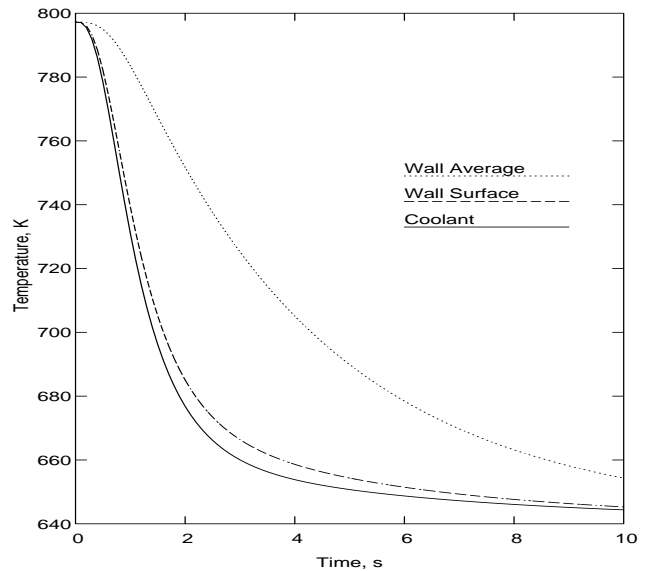


Fig. 4, Coolant and Structure Temperatures at the Above Core Load Pads of a Sodium Cooled ATW Following a Beam Interruption

The coolant and structure temperatures at the top of the core are shown in Figure 6 for the lead-bismuth cooled version of ATW. In this case the structure surface temperature does not follow the coolant temperature as closely as in the sodium coolant case, since the thermal

conductivity of lead-bismuth is significantly lower than that of sodium.

The temperature differences across the structure are smaller. Without accounting for additional fatigue from return to power, the subassembly duct wall will last 4.8 years in the lead-bismuth case.

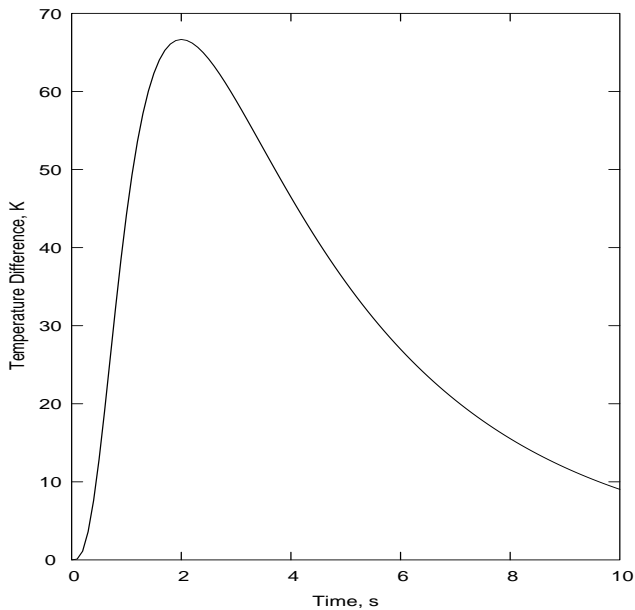


Fig. 5, Difference Between the Structure Average Temperature and the Structure Surface Temperature at the Above Core Load Pads of a Sodium Cooled ATW

The impact of a sudden return to power twenty seconds after a beam interruption is shown in Figure 7 for the above core load pads in the sodium cooled case. The structure surface temperature drops rapidly after the beam interruption and rises rapidly after the return to power. The average structure temperature lags behind the surface temperature. Figure 8 shows the difference between the structure average temperature and the structure surface temperature for this case. The return to power gives a curve that is a mirror image of the transient due to the interruption. In this case, the peak structure temperature difference that enters into the thermal fatigue calculation is twice as high as it would be with no return to power. This would reduce the component lifetime to 3 days.

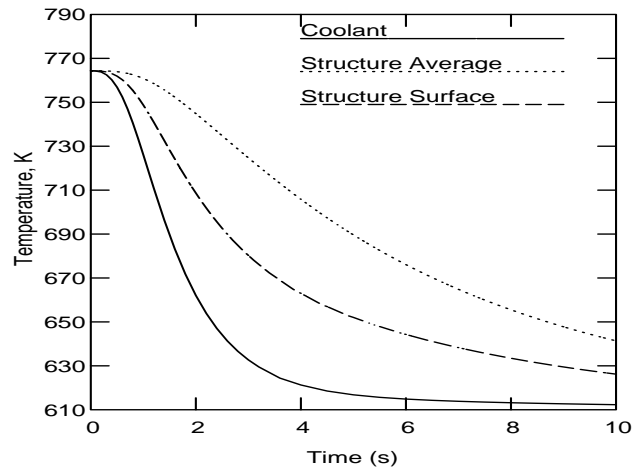


Fig. 6, ATW Above Core Load Pad Temperatures after a Beam Interruption, Pb-Bi Case

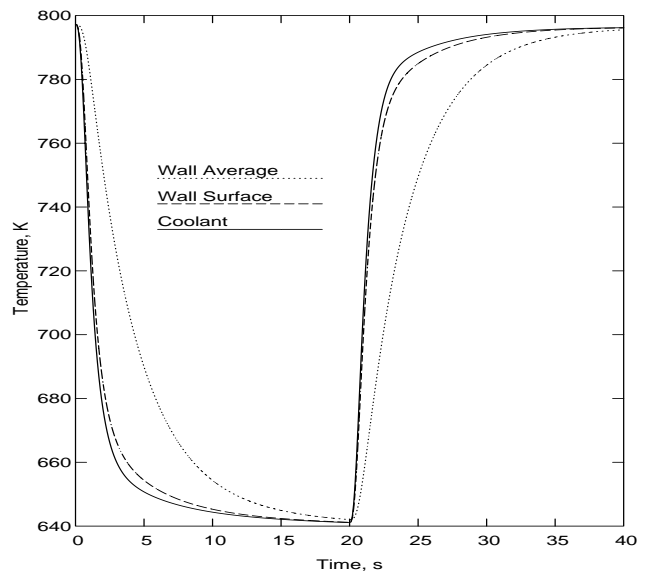


Fig. 7, Coolant and Structure Temperatures at the Above Core Load Pad of a Sodium Cooled ATW Due to a Sudden Return to Power After a 20 Second Beam Interruption

The results in Figure 8 demonstrate the need to return to power gradually rather than suddenly after a beam interruption. This topic has been investigated for the third multiplier concept, the sodium cooled ADTF. In this design there are no above core load pads on the subassembly walls. Instead there are dimples in

the duct wall to provide spacing between subassemblies. The duct walls and dimples are thin enough that thermal fatigue is not an issue with them. Instead, what is an issue is the thick neutron shielding inside the subassemblies and above the core. Thermal fatigue cracks in this shielding may not matter if the material stays in place. On the other hand if cracked pieces move and block coolant channels then the cracks will matter a lot.

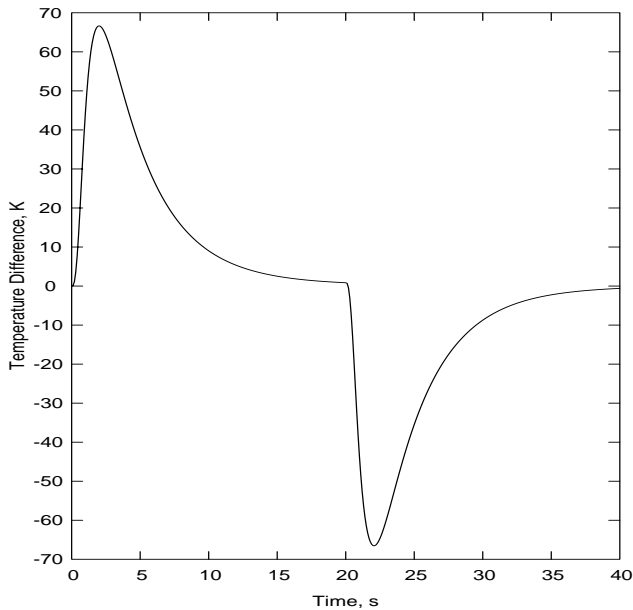


Fig. 8, Average Structure Temperature Minus Structure Surface Temperature at the Above Core Load Pad of a Sodium Cooled ATW Due to a Sudden Return to Power After 20 Seconds

Figure 9 shows the structure temperature differences in the above core shielding for a beam interruption of 10 seconds followed by a ramp back to power with various ramp rates. An immediate return to power adds 40 K to the amplitude of the temperature transient. Even a 300 second ramp adds a few degrees to the amplitude.

The tubes going through the tube sheets of the IHX are spaced fairly close together, so when there is a temperature transient and the tube side coolant changes temperature the bulk of the interior of the tube sheet responds fairly rapidly and uniformly. On the other hand, at the

outer edge of the tube sheet there is a fairly wide rim with no tube penetrations. The outer rim temperatures respond more slowly to temperature transients, leading to thermal strains in the outer rim. Figure 10 shows the difference between the outer rim temperature and the interior temperature for the upper tube sheet rim for a beam interruption of 1000 seconds followed by a ramp back to power. The time scales in this case are much longer than in previous cases. Even a 16000 second ramp back to power adds more than 10 K to the amplitude of the transient.

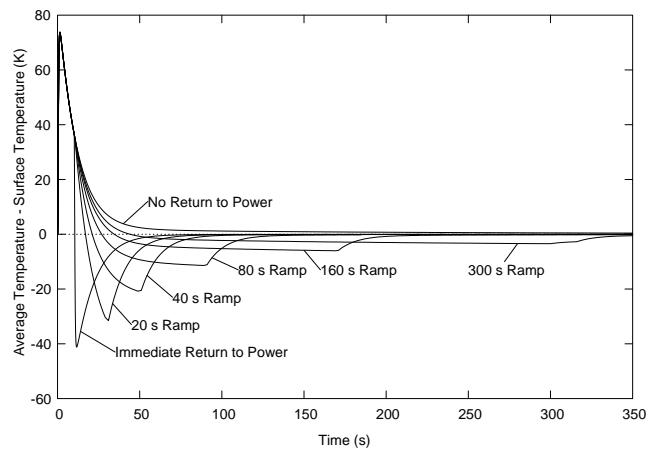


Fig. 9, Structure Temperature Differences in the Above Core Shielding of the ADTF Due to a Beam Interruption of 10 Seconds, Followed by a Ramp Back to Power

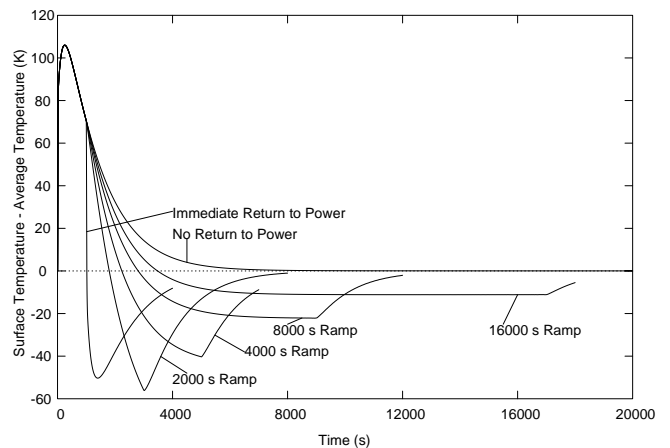


Fig. 10, Structure Temperature Differences in the IHX Tube Sheet Rim of ADTF Due to a Beam Interruption of 1000 Seconds, Followed by a Ramp Back to Power

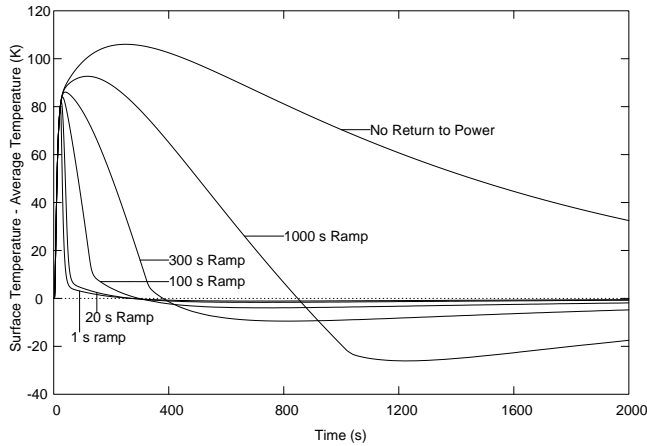


Fig. 11, Structure Temperature Differences in the IHX Tube Sheet Rim of ADTF Due to a Beam Interruption of 20 Seconds, Followed by a Ramp Back to Power

Figure 11 shows the structure temperature differences in the IHX upper tube sheet rim for a beam interruption of 20 seconds, followed by a ramp back to power. In this case the return to power starts before the temperature peak, and a rapid return to power is advantageous.

V. RETURN TO POWER SCHEMES

There is a conflict between specifying a return to power scheme to protect short time constant structures and specifying a scheme to protect long time constant structures. In the ADTF temperature differences in the above core shielding peak 1.4 seconds after an interruption, whereas temperature differences in the IHX tube sheet rim do not peak until 250 seconds after the interruption. For an interruption with a duration greater than 1.4 seconds but significantly less than 250 seconds, after the interruption one would want to return to power slowly to minimize the additional thermal fatigue in the above core shielding; but one would want to return to power quickly to minimize the peak temperature difference in the IHX tube sheet rim. Some compromise is necessary. Results obtained with two different return to power schemes are presented below to quantify the effects of this conflict.

Scheme A for Return to Power After a Beam Interruption

Interruption < 1 second	return to power immediately, if possible
1 s ≤ interruption < 50 s	ramp time = 300 seconds for return to power
50 s ≤ interruption < 400 s	double ramp, 0-.75 power in 300 seconds
	.75 – 1.0 power in 8000 more seconds
interruption ≥ 400 s	ramp time = 16,000 seconds

Scheme B for Return to Power After a Beam Interruption

Interruption < 1 second	return to power immediately, if possible
1 s ≤ interruption < 50 s	ramp time 100 seconds for return to power
50 s ≤ interruption < 400 s	double ramp, 0 - .75 power in 100 seconds
	.75 – 1.0 power in 8000 more seconds
interruption ≥ 400 s	ramp time = 16,000 seconds

Table 2, Component Lifetimes, Impact of Return to Power Scheme

Component	Lifetime (years), ignoring temperature overshoot from return to power	Lifetime (years), scheme A	Lifetime (years), scheme B
IHX upper tube sheet rim	1.01	.48	.69
Above core shielding	.40	.26	.15

The difference between these two return to power schemes is that for short interruptions the ramp time in scheme B is 100 seconds instead of 300 seconds. Thus, scheme A provides more protection to the above core shielding, whereas scheme B provides more protection to the IHX upper tube sheet rim.

VI. MITIGATION MEASURES

The component lifetimes in Table 2 are unacceptable. The subassemblies are left in the core for three or four years, so an above core shielding lifetime of at least three or four years is required. The lifetime of the IHX should be at least as long as the expected operational lifetime of the plant, although replacing the IHX once during the plant lifetime may be acceptable. Replacing the IHX would be expensive. Thus, some mitigation measures need to be taken to reduce accelerator beam interruptions and/or to increase the tolerance of the blanket to beam interruptions.

As mentioned above, a significant reduction in the frequency of beam interruptions should be possible. A new accelerator built with modern technology would be expected to be more reliable than LANSCE by a factor of ten or more. A factor of ten increase in component lifetime would be helpful but not sufficient. Additional improvement is necessary.

Increasing the tolerance of the blanket to beam interruptions requires design changes. Either the thicknesses of critical structural materials must be reduced or transient temperature changes must be reduced. An example of a SCM-100 design in which the transient temperature changes are reduced is given below.

VII. A BEAM INTERRUPTION TOLERANT DESIGN

The ADTF SCM-100 results presented here so far were for a design which is basically the EBR-II reactor scaled up from 62.5 MWt to 100 MWt by increasing the number of subassemblies in the core and increasing the number of tubes in the IHX. The average coolant flow per subassembly and the average power per subassembly were approximately the same in the scaled up version. Also, the coolant temperature rise across the intermediate side of the IHX was similar. In the upper tube sheet rim of the IHX, the magnitude of the temperature perturbations caused by a beam interruption depends mainly on the IHX intermediate side coolant temperature rise. On the other hand, the magnitude of the temperature perturbations in the above core shielding depends mainly on the primary coolant temperature rise across the blanket subassemblies. Therefore, in the modified, more tolerant SCM-100 design both the primary and the intermediate coolant flow rates were increased to reduce coolant temperature rise.

Table 3 lists some of the relevant design and operating parameters of the modified SCM-100. Parameters for the original design and for EBR-II at the time of the SHRT-17 test are also listed for comparison. For the modified design, the total power and the number of driver subassemblies were held constant while the coolant flow per subassembly was increased about 25%. The same thermal fatigue result could have been achieved by holding the total power and the coolant flow rate per subassembly constant and increasing the number of driver subassemblies by about 25%.

In order to make use of the spare EBR-II IHX, two EBR-II IHXs were used in the modified design. The original design used one new IHX similar to but larger than the EBR-II

IHX. It would probably be possible to achieve satisfactory thermal fatigue results with a single EBR-II IHX if the total primary and secondary coolant flows were the same as in this modified design, but the IHX pressure drops would be much higher. Thus, there may be a trade-off between paying more money for IHXs or paying

more money for larger pumps. Also, note that the modified SCM-100 design is more expensive than the original design, especially in the requirement for larger pumps. In general, design modifications to increase tolerance of beam interruptions increase the cost of the multiplier.

Table 3, ADTF SCM-100 and EBR-II Design and Operating Parameters

	EBR-II	SCM-100 Original	SCM-100 Modified
Power (MWt)	62.5	100	100
Average coolant temperature rise in the core (K)	97	101	81
Peak coolant temperature rise in the hottest subassembly (K)	132	120	96
IHXs	1	1	2
Tubes per IHX	3248	5197	3248
Active length of IHX (m)	3.16	3.16	3.16
IHX intermediate flow/primary flow	.71	.68	1.0
Temperature rise across intermediate side of IHX (K)	139	148	81
Primary centrifugal pumps	2	2	2
Intermediate pumps	1	1	2
Pump head, primary (bar)	3.22	2.93	4.20
Pump flow, primary (Kg/s/pump)	242	409	511
Pump head, intermediate (bar)	3.64	4.68	7.93
Pump flow, intermediate (Kg/s/pump)	326	528	482

Table 4, Structural Component Lifetimes

Component	Lifetime (years) original design	Lifetime (years) modified design
IHX upper tube sheet rim	.48	13.1
Above core shielding	.26	4.9

Table 4 lists the component lifetimes for the modified SCM-100 design, using Eriksson's beam interruption frequency results and using return to power scheme A. Results for the original design are also listed for comparison. The above core shielding lifetime of 4.9 years should be adequate, since subassemblies are normally replaced after three or four years. The upper tube sheet rim lifetime will be adequate if there is any significant improvement (a factor of two or more) in beam reliability.

VIII. CONCLUSIONS

A beam trip in an accelerator driven system leads to a rapid temperature transient that contributes to thermal fatigue in various structural components of the multiplier. Going back up to power contributes additional thermal fatigue. In an accelerator driven system using an accelerator with the reliability of the LANSCE accelerator and using a multiplier not specifically designed to tolerate large numbers of beam interruptions the lifetimes of some structural components would be unacceptably small. A significant improvement in accelerator reliability would be expected with a modern accelerator. If the improvement in accelerator reliability is not enough, then the multiplier

design can be modified to tolerate more beam interruptions. The multiplier modifications would add to the cost of the multiplier.

Utilization and Reliability of High Power Accelerators, MITO, Japan (October 13-15, 1998).

IX. ACKNOWLEDGEMENTS

This work was supported by the United States Department of Energy under contract No. W-31-109-ENG-38.

REFERENCES

1. P. M. Magee, A. E. Dubberley, A. J. Lipps and T. Wu, "Safety Performance of the Advanced Liquid Metal Reactor," *Proceedings of ARS '94 International Topical Meeting on Advanced Reactors Safety*, Pittsburg, Pennsylvania, Vol. 2, pp. 826-833 (April 1994).
2. *A Roadmap for Developing Accelerator Transmutation of Waste (ATW) Technology*, A Report to Congress, DOE/RW-0519 (October 1999).
3. F. E. Dunn, F. G. Prohammer, D. P. Weber and R. B. Vilim, "The SASSYS-1 LMFBR Systems Analysis Code," *ANS International Topical Meeting on Fast Reactor Safety*, Knoxville, TN, pp. 999-1006 (April 1985).
4. The American Society of Mechanical Engineers, *1998 ASME Boiler & Pressure Vessel Code, an International Code*, Section III, Subsection NH, Appendix T, Article T-1432.
5. M. Eriksson et al., "Reliability Assessment of the LANSCE Accelerator System," *Proc. Workshop on the*